NEW PROCEDURE TO CALCULATE COMPRESSION STRENGTH OF FRP USING THE SERIAL/PARALLEL MIXING THEORY

Xavier MARTINEZ [1] Sergio OLLER [1] Alex BARBAT [1] Fernando RASTELLINI [1]

[1] Departament de Resistencia de Materials i Estructures a l'Enginyeria (RMEE) – International Centre of Numerical Methods in Engineering (CIMNE), Polytechnic University of Catalonia (UPC), Barcelona, Spain

Keywords: compression strength, fibre buckling, FRP reinforcement, micro-model, serial/parallel mixing theory.

1 INTRODUCTION

The use and applications of fibre reinforced polymers (FRP) to reinforce and retrofit existing structures has increased exponentially in last decades. Nowadays, these composite materials can be found as tensile reinforcements, shear reinforcements, column wrapping, etc. Although FRP reinforcements are not recommended to be used to resist compressive forces (Rabinovich [1]), there are many situations in which this load state can be found. This aspect is of special relevance in the case of structures subjected to seismic loads, where the sign of the load is reversed as the earthquake evolves, in case of fatigue loads or when a strengthened element is unloaded. Thus, a procedure to obtain the compression strength of FRP composites is required in order to take into account this sort of situations.

The main failure cause of compressed FRP is the fibre buckling phenomenon. Fibres are very slender elements and their second order effects are avoided by the matrix elastic restrain. However, as damage in matrix evolves, fibre restrain becomes weaker and fibre buckling occurs.

First studies about fibre buckling correspond to Rosen [2], who defined two different buckling modes: extensional and shear buckling. He also defined the compression stress at which this buckling occurs. This stress value is defined by the matrix shear strength and by the amount of fibres found in the composite. From this initial approximation, different authors have developed new models in order to obtain a better prediction of composite compression strength due to fibre buckling. Among different existing studies, it is worth to mention the works by Barbero and Tomblin [3], Balacó de Morais and Torres Marques [4] and Drapier *et al.* [5]. All these authors consider composites as a single orthotropic material. Using energetic equilibrium, they develop micro-mechanical models from which the final compression stress in the composite is obtained. The expressions found in all different models agree in the dependence of the critical compression stress on three main parameters: *(a)* Matrix shear strength, *(b)* Fibre initial misalignment and *(c)* Proportion between fibre and matrix in the composite. Hence, the limit compression stress of these new formulations depends on the same parameters pointed out by Rosen and on a new one: fibre initial misalignments. According to Jochum and Grandidier [6], fibre misalignments are produced in the composite manufacturing process, during the matrix curing. These misalignments are regular along the whole fibre and can be represented by a sinusoidal shape.

The fibre buckling formulation proposed in this paper appears in the context of FRP reinforcement and retrofitting simulations using numerical techniques. These simulations are made using a finite element code which deals with composite materials using the serial/parallel rule of mixtures developed by Rastellini [7]. This theory allows obtaining the composite behaviour from the response of its constituents, each one computed with its own constitutive law. The developed simulations have proved the accuracy of the proposed numerical method, which is able to obtain the different effects produced by different FRP reinforcements in the same structure, the behaviour of the structure if it is reinforced or if it is retrofitted, etc. The code has been validated using experimental values. Some of the simulations realized are exposed in Martinez *et al.* [8].

This paper includes a brief description of the serial/parallel (S/P) rule of mixtures as well as its use in the simulation of FRP reinforcements of existing structures. Afterwards, the new formulation proposed to obtain the compression strength of composite materials is exposed. Finally, the new formulation is validated.

2 NUMERICAL SIMULATION OF FRP REINFORCEMENTS USING THE SERIAL/PARALLEL RULE OF MIXTURES

2.1 Serial/Parallel Rule of Mixtures

The serial parallel rule of mixtures is implemented in PLCd code. This is a finite element code developed at the Polytechnic University of Catalonia (UPC). The code works with two and three dimensional finite elements, has many constitutive laws to predict the material behaviour (Von-Mises, Mohr-Coulomb and Drucker-Prager among others) and different integration algorithms to simulate the material evolution (damage, plastic damage, visco-elasticity, etc). It can also perform dynamic simulations using the Newmark method.

The classical mixing theory was first developed by Trusdell and Toupin [9]. It supposes that all constituent materials included in a structural point have the same strain values. This is a major limitation because only composite materials whose constituents present a parallel behaviour can be considered. The S/P rule of mixtures corrects this situation, being able to deal with composites with serial and serial//parallel behaviour. Fig. 1 shows the composite components distribution corresponding to all these situations.

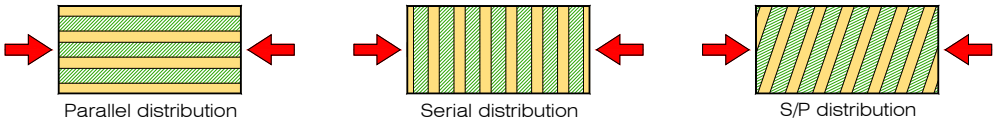

Fig. 1 Distribution of components in a composite material

The serial/parallel rule of mixtures, developed by Rastellini [7], considers that in a certain direction the compounding materials behave in parallel, while their behaviour is in serial in the remaining directions. In the case of fibre reinforced polymers, the parallel direction corresponds to the fibre direction. The numerical model is based on the following hypotheses:

1. The component materials have the same strain in parallel (fibre) direction
2. The component materials have the same stress in serial direction
3. The composite response is in direct relation with the volume fractions of component materials
4. A homogeneous distribution of phases is considered in the composite
5. A perfect bounding between components is also considered

With these hypotheses, the implemented algorithm employs the split of serial and parallel parts of the stress and strain tensors. Thus,

$$\varepsilon_P = P_P : \varepsilon; \qquad \varepsilon_S = P_S : \varepsilon; \qquad \varepsilon = \varepsilon_P + \varepsilon_S \tag{1}$$

$$\sigma_P = P_P : \sigma; \qquad \sigma_S = P_S : \sigma; \qquad \sigma = \sigma_P + \sigma_S \tag{2}$$

being P_P and P_S the parallel and serial projector tensors (respectively). The equations that establish the strain compatibility between components arise from the analysis of the hypotheses previously exposed. Defining the superscript $i = c, m, f$ as composite, matrix and fibre respectively, and ${}^{i}k$ as the volumetric participation in the composite of each component, the compatibility equations can be written as:

Parallel behaviour:

$$\begin{aligned} {}^{c}\varepsilon_P &= {}^{m}\varepsilon_P = {}^{f}\varepsilon_P \\ {}^{c}\sigma_P &= {}^{m}k \cdot {}^{m}\sigma_P + {}^{f}k \cdot {}^{f}\sigma_P \end{aligned} \tag{3}$$

Serial behaviour:

$$\begin{aligned} {}^{c}\varepsilon_S &= {}^{m}k \cdot {}^{m}\varepsilon_S + {}^{f}k \cdot {}^{f}\varepsilon_S \\ {}^{c}\sigma_S &= {}^{m}\sigma_S = {}^{f}\sigma_S \end{aligned} \tag{4}$$

The first operation performed by the algorithm implemented in PLCd code is to split the strain tensor into its parallel and its serial parts, in order to compute the strain state in matrix and fibre materials. The parallel strain component is, according to equation (3), the same for both materials and

for the composite. On the other hand, the serial strain component requires a first prediction of the strains expected in one of the composite components. This prediction is done in matrix material. Once the strain state is known, the stress tensor of matrix and fibre materials is computed using their own constitutive law:

$$\begin{aligned} {}^{m}\sigma &= {}^{m}C : ({}^{m}\varepsilon - {}^{m}\varepsilon^{p}) \\ {}^{f}\sigma &= {}^{f}C : ({}^{f}\varepsilon - {}^{f}\varepsilon^{p}) \end{aligned} \tag{5}$$

where ${}^{i}C$ is the constitutive tensor of fibre and matrix and ${}^{i}\varepsilon^{p}$ the plastic strain tensor. The two stress tensors computed with equation (5) must fulfil the equilibrium equations. This means that the matrix serial stresses must be equal to the fibre serial stresses (equation(6). A Newton Raphson scheme is applied to reduce the stress residue and to correct the initial prediction of matrix serial strains until equation (6) is verified.

$$\left[\Delta\sigma_S\right]^k = \left[{}^{m}\sigma_S\right]^k - \left[{}^{f}\sigma_S\right]^k \leq \text{toler} \tag{6}$$

2.2 Simulation of FRP reinforcements using the code

In this section, a numerical simulation of a bending reinforced beam is presented. This case shows the efficiency of the serial/parallel rule of mixtures to deal with this sort of structural problems, as it is able to reproduce the complex mechanical behaviour found in the beam with an acceptable computational cost. The numerical results are validated with experimental values. The studied beam is defined in the paper by Spadea *et al.* [10]. Its geometry and the reinforcements applied to it are shown in Fig. 2

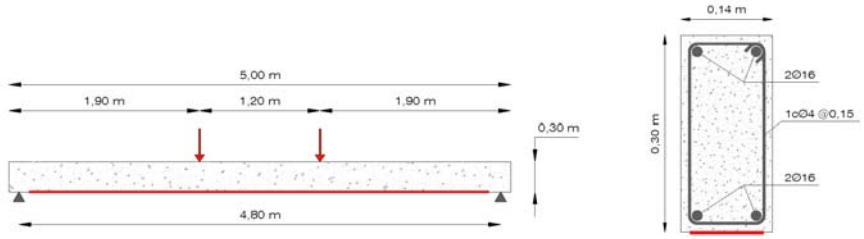

Fig. 2 Geometry and reinforcement of the beam studied

The red (thick) line displayed in the bottom of the beam corresponds to the FRP reinforcement. This is made of carbon fibres embedded in a polymeric matrix. The content of fibres is 60% and the composite thickness is 1.2 mm. The finite element model developed to simulate the beam reinforcement is shown in Fig. 3. This is a 3D finite element made with linear hexahedrons.

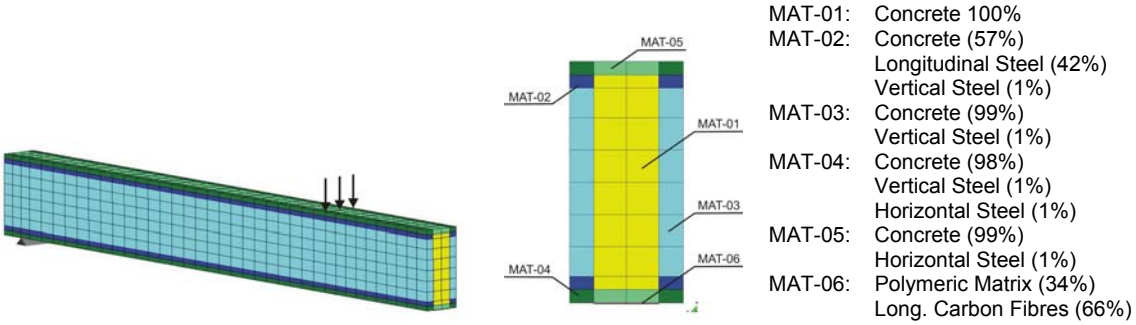

Fig. 3 Finite element model developed to realize the numerical simulation

The usage of the S/P rule of mixtures allows considering all the reinforcement details found in the beam using a coarse mesh. In Fig. 3 it is also included the composite materials composition. As can be seen, a single finite element contains, in this particular case, up to three different component materials. The steel reinforcements are considered as fibres, whose orientation is defined by the bar

direction. The FRP reinforcement has been included adding new finite elements to reproduce with more accuracy its position in the beam.

The results obtained with this simulation are compared with the experimental results reported by Spadea *et al.* [10]. Fig. 4 shows the vertical displacement of the beam, in the point where the force is applied, against the load value. This figure demonstrates the agreement between numerical and experimental results, which proves the ability of the method to perform this sort of simulations. Fig. 4 also includes the results obtained with a numerical simulation of the same beam without FRP reinforcements. The comparison between the results obtained for the reinforced and for the non-reinforced beam shows the improvement obtained in the beam performance when it is reinforced with FRP.

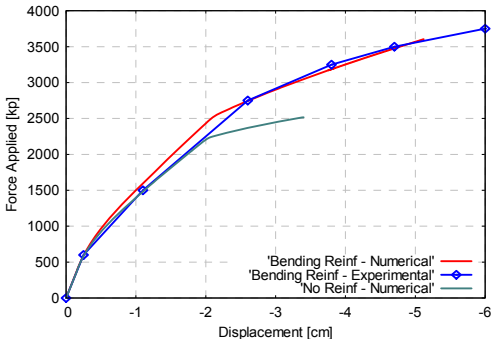

Fig. 4 Force-displacement graph comparing the experimental and the numerical results

One of the main advantages of the proposed finite element formulation is that it allows obtaining the structural behaviour of all its components, their failure causes, their strain-stress state, etc. In Fig. 5 some results maps, corresponding to the final computed step, are represented. These show the most relevant information obtained from the numerical simulation. Fig. 5a displays the plastic damage in concrete, which shows that the failure cause of the beam are the tensile stresses in concrete at midspan. In Fig. 5b and Fig. 5c it is depicted the plastic damage obtained for the longitudinal steel reinforcement and for the polymeric matrix, respectively. These two figures show that both materials have reached their yield stress when the beam failure occurs. Finally, Fig. 5d shows the stresses in carbon fibres. As it can be seen, they are at less than a half of their load capacity (the fibre elastic limit stress defined is: $\sigma^e = 2300$ MPa)

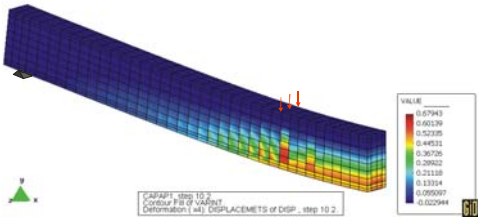

Fig. 5a Plastic damage in concrete

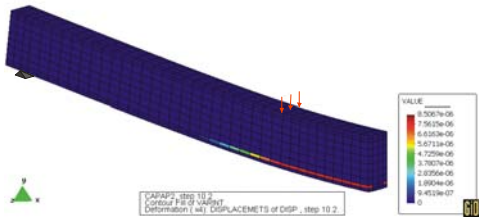

Fig. 5b Plastic damage longitudinal steel reinf.

Fig. 5c Plastic damage in polymeric matrix

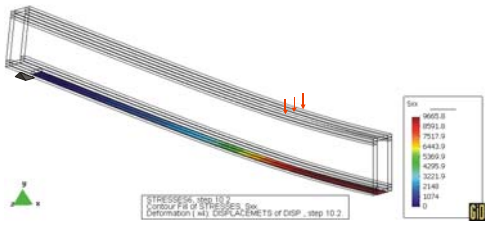

Fig. 5d Longitudinal stresses in carbon fibres [kp/cm^2]

Fig. 5 Results maps obtained with the finite element model of the beam

3 MICRO-FORMULATION TO OBTAIN COMPRESSION STRENGTH OF COMPOSITES

3.1 Approach used in solving the fibre buckling problem

In all existing bibliography, the fibre buckling problem is solved by using different methodologies to obtain a general expression for the composite limit compression stress. This expression is only valid

for the composite material and is obtained taking into account different characteristics of the composite components. Alternatively, in the present work, the composite material will be modelled using the S/P rule of mixtures. Thus, the fibre buckling problem must be solved in terms of the composite components, considering their interaction, and not in terms of the composite by itself.

The interaction between fibres and matrix appears when the composite is compressed: matrix restrain fibres avoiding their transversal movement. Under this approach, matrix can be considered as an elastic restriction of fibres, and the fibre-matrix system can be represented as it is shown in Fig. 6. In this figure the movement of the fibres in case of compression has been represented in dashed lines. Fibre behaviour is analogous to the response that is obtained in a curved bar under unilateral restrain. This analogy is used to formulate the fibre buckling problem.

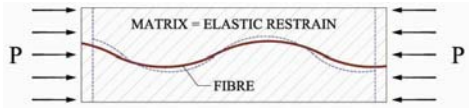

Fig. 6 Fibre-matrix system. Fibre behaviour when the composite is compressed

According to Fig. 6, the fibre stiffness is reduced due to its original misalignment: for a fixed value of P, fibre longitudinal strain is increased due to its structural deformation. The deformation suffered by fibres is directly related to matrix elastic modulus, which is reduced when damage evolves in matrix material. As matrix damage increases, fibre restrain becomes lower and its stiffness decreases. Hence, the problem will be solved introducing a varying elastic modulus in fibres, dependent on the matrix damage internal variable and on the fibre initial misalignments. Fibre buckling will occur when matrix cannot restrain fibres anymore. Proceeding in this way, the parameters defined in literature in which the problem depends (matrix shear strength, fibre misalignments and proportion between fibre and matrix) are considered in the resolution process. The first two parameters are included in the calculation of fibre modified elastic modulus and the last parameter is included in the rule of mixtures, as composite behaviour depends on the volumetric participation of its components.

3.2 Equations of a curved bar under unilateral restriction

The equations that define the behaviour of a curved bar under unilateral restriction were developed by Hetény in [11]. Considering the curved bar displayed in Fig. 7a, the equations that define its behaviour are obtained studying the equilibrium of forces of an infinitesimal section (Fig. 7b). The elastic restriction of the beam is considered as a radial load (q) dependent on fibre radial displacement (ω) and the matrix elastic modulus (k).

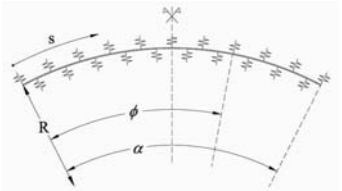

Fig. 7a Curved bar geometry

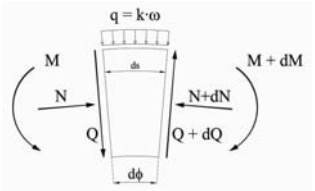

Fig. 7b Forces acting on an infinitesimal section

Fig. 7 Curved bar under unilateral restriction problem

The equilibrium of forces displayed in Fig. 7b defines the following equations:

$$\begin{aligned} q\,ds - N\,d\phi &= dQ \\ Q\,d\phi &= dN \\ Q\,R\,d\phi &= dM \end{aligned} \qquad (7)$$

Neglecting the axial deformation of the bar due to the normal force N , the differential bending equation of a circular arch of radius of curvature R and flexural rigidity EI is:

$$\frac{EI}{R^2}\left(\frac{d^2\omega}{d\phi^2}-\omega\right)=-M \tag{8}$$

Rearranging equations (7) and (8), the bar displacement in its radial directions defined by the differential equation:

$$\frac{d^5\omega}{d\phi^5}+2\frac{d^3\omega}{d\phi^3}+\eta^2\frac{d\omega}{d\phi}=0 \tag{9}$$

where $\eta=\sqrt{\frac{R^4k}{EI}+1}$

The general solution of equation (9) is:

$$\begin{aligned}\omega = \; & C_0 \; + \; \left[C_1\cosh(\eta_1\phi)+C_2\sinh(\eta_1\phi)\right]\cos(\eta_2\phi) \\ & + \; \left[C_3\cosh(\eta_1\phi)+C_4\sinh(\eta_1\phi)\right]\sin(\eta_2\phi)\end{aligned} \tag{10}$$

with $\eta_1=\sqrt{\frac{\eta-1}{2}}$ and $\eta_2=\sqrt{\frac{\eta+1}{2}}$

To obtain the particular solution for the curved bar problem, some boundary conditions must be imposed. Defining the axis of symmetry as the origin of angle ϕ, two boundary conditions can be defined (11). These two conditions force the integration constants C_2 and C_3 to be zero. The rest of boundary conditions are obtained according to the fibres structural model. This is depicted in Fig. 8 and the boundary conditions to be applied are described in figure Fig. 9.

$$\left.\frac{d\omega}{d\phi}\right|_{\phi=0}=0 \qquad Q(\phi=0)=0 \tag{11}$$

Fig. 8 Fibres structural model

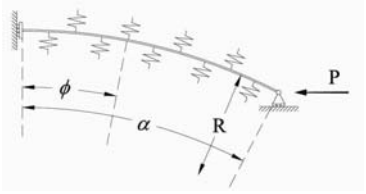

1st B.C. $M(\phi=\alpha)=0$

2nd B.C. $N(\phi=\alpha)\cos\alpha-Q(\phi=\alpha)\sin\alpha=P$

3rd B.C. $v(\phi=\alpha)=0$

being v the vertical displacement of the bar.

Fig. 9 Boundary conditions to apply to fibre structural model

3.3 Fibre modified elastic modulus due to fibre buckling

The equations shown in previous section allow obtaining the structural displacement of fibres due to its original misalignment. This displacement does not take into account the displacement produced by longitudinal strains due to the compression force applied to the structure. As the objective sought is to use this displacement to modify fibres elastic modulus, it has to be transformed into strains. This can be done dividing the displacement obtained by the bar length.

$$\varepsilon^{cb} = \frac{u}{l} = \frac{u}{R\sin\alpha} \tag{12}$$

where u is the horizontal bar displacement, for $\phi = \alpha$, obtained when solving the curved bar under unilateral restrain problem. Structural strains due to fibre misalignments must be added to the normal strains due to the compression force applied to the fibres (ε^P). Thus, the total longitudinal strain that will be found in fibre material is:

$$\varepsilon = \varepsilon^P + \varepsilon^{cb} = \frac{P}{AE} + \frac{u}{R\sin\alpha} \tag{13}$$

being A fibre area, E its elastic modulus and P the horizontal force applied to solve the curved bar problem. To obtain the total strain straightforward, the elastic modulus of fibres is replaced by the fibre modified elastic modulus, which is obtained as:

$$\hat{E} = \frac{P/A}{P/AE + u/R\sin\alpha} \tag{14}$$

Equation (14) shows that the fibre modified elastic modulus varies in function of the fibre initial misalignments and in function of the matrix stiffness, as the value of u depends on these two parameters. $\hat{E}$ will remain constant while matrix is under elastic conditions and, as soon as damage in matrix starts, its elastic modulus will vary and so will do $\hat{E}$.

3.4 Numerical implementation of fibre modified elastic modulus

Fibre modified elastic modulus is computed in two different places of the finite element code. The first one is at the beginning of the code, where the modified elastic modulus replaces the fibres original one. In this way, the behaviour of fibres due to their original misalignment can be taken into account along the whole calculation process. The second place where the fibre elastic modulus is computed is into the rule of mixtures algorithm. After obtaining the matrix stress tensor, it is possible to know if the matrix material has reached its elastic limit stress and if damage has occurred. In this case, fibres elastic restrain is modified and a new modified elastic modulus must be obtained. Proceeding in this way, fibres are always computed according to the matrix state. The algorithm of this numerical implementation is displayed in Fig. 10.

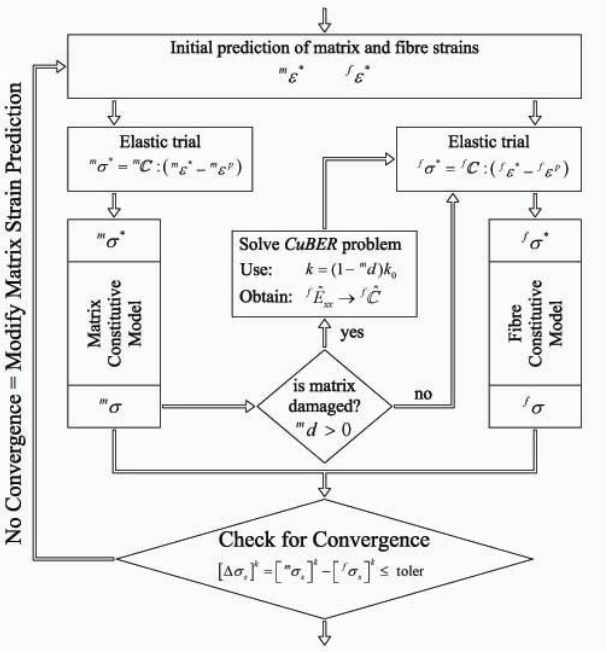

Fig. 10 Numerical implementation of modified elastic modulus in the S/P rule of mixtures algorithm

4 VALIDATION OF COMPUTATIONAL METHOD

The validation of the computational method has been done comparing the compression load obtained with the new formulation developed in this paper with the experimental results described in the paper of Barbero and Tomblin [3] in which twelve different composites have been tested to obtain their compression strength. The different composites are made of glass fibres in a polymeric matrix and each one is characterized by the kind of fibres and polymer used and the fibre volume content. Fibre misalignment has been measured for each sample. The validation has been realized using three of these samples which characteristics are exposed in Table 1. The mechanical characteristics considered for each component material are described in Table 2.

Table 1 Materials composing the samples modelled.

Sample	Matrix material	Fibre material	Fibre volume fraction	Misalignment expected angle
CAA	Polyester 2036C	Glass-fibre OC 102-AA-56	40 %	2.76º
CBB	Vinyl Ester D-1419	Glass-fibre OC 366-AD-113	43 %	2.87º
ACA	Polyester 2036C	Glass-fibre OC 102-AA-56	55 %	2.63º

Table 2 Mechanical properties of the materials composing the samples.

Material	Limit strength [MPa]	Elastic modulus [GPa]	Poisson modulus	Fracture energy [m·Pa]
Glass fibre	1800	75,0	0,20	1000
Polyester matrix	35	3,0	0,35	15
Vinyl ester matrix	40	3,5	0,35	18

Glass fibre OC 102-AA-56 has a diameter of 13 μm and OC 366-AD-113 has a diameter of 23 μm. The misalignment expected corresponds to the half normal distribution of all the angle misalignments measured for each sample. To obtain the shape of fibre misalignments from this angle, the result obtained by Jochum and Grandidier [6] are used. These say that the amplitude found in the fibre misalignments corresponds to 1 to 2 times the fibre diameter. Thus, an amplitude of 15 and 25 μm will be considered respectively for the two kind of fibres described. Using the misalignment expected angle, according to Fig. 11, the amplitude and wave-length for each sample is

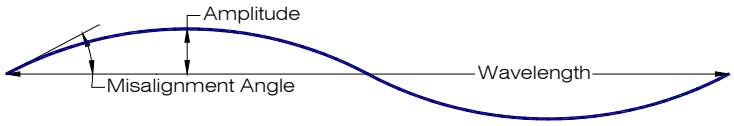

Fig. 11 Geometry of fibre misalignments considered

CAA: Amplitude: 15 μm Wavelength: 1244 μm
CBB: Amplitude: 25 μm Wavelength: 1994 μm
CAA: Amplitude: 15 μm Wavelength: 1306 μm

The experimental fibre buckling compression stress found by Barbero and Tomblin [3] for each one of these composites is shown in Table 3.

Table 3 Fibre buckling experimental compression stress found in each composite sample.

	CAA	CBB	ACA
Limit Compression Stress	477.74 MPa	521.56 MPa	560.90 MPa

Three different numerical simulations have been developed, each one corresponding to one of the samples previously defined. All of them have been computed with the finite element model shown in Fig. 12, modifying their material definition according to the composites defined by Barbero and Tomblin.

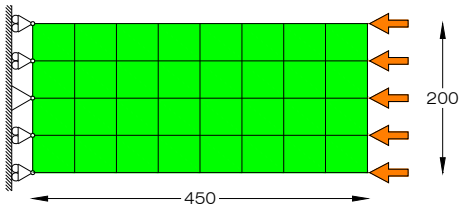

Fig. 12 Models Developer to validate the code. The dimensions are in μm

The results obtained with each model are displayed in Fig. 13, where the force applied to the finite element structure is plotted against the displacement in the face where the load is applied. In this figure the forces that would be required in the structure, for the maximum compression stress obtained with the experimental simulation, have been also included. The relative error obtained in each numerical model shows the good performance of the formulation proposed.

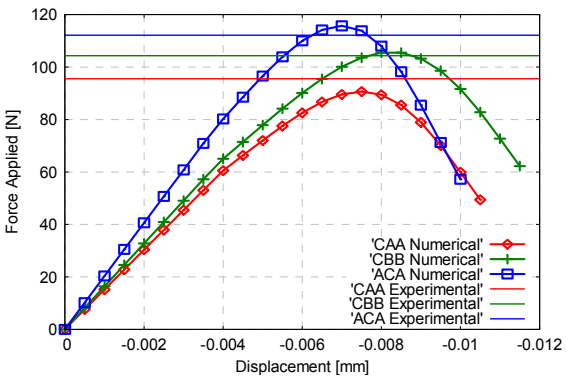

Relative error obtained in each sample:

CAA: 5.1%
CBB: 1.1%
ACA: 3.1%

Fig. 13 Comparison among experimental and numerical results

The different compression strength values obtained for each composite show the dependence of the formulation on the value of fibre initial misalignments, on matrix characteristics and on the volumetric participation of fibres and matrix in the composite, as these parameters differentiate the three composites considered in the numerical simulation.

The composite capacity due to fibre misalignments is compared with the maximum compression that can be applied to it if no misalignments are considered (Fig. 14). As it can be seen, fibre misalignments reduce compression capacity in more than a 30% in the case considered. If fibre strength is larger, i.e. when carbon fibres are used, this reduction will be also larger.

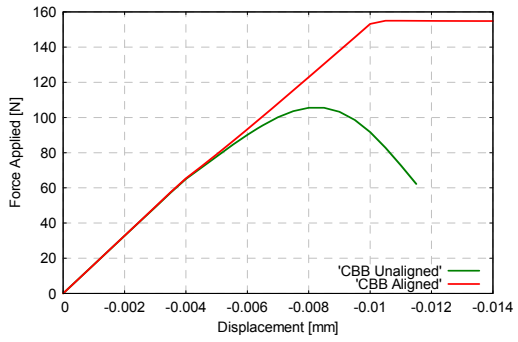

Fig. 14 Compression strength with aligned and unaligned fibres

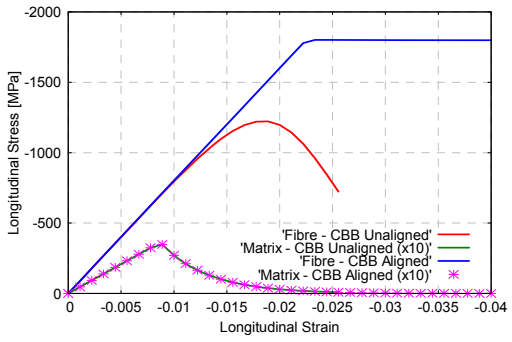

Fig. 15 Composite components behaviour. Stress-strain diagram

The strength reduction shown in Fig. 14 is explained comparing the composite components behaviour obtained with both models. Fig. 15 shows the longitudinal stress-strain diagram for fibre and matrix. Matrix stresses have been scaled by 10 to see better in the graph their evolution. When no misalignment is considered, matrix and fibre stress evolution are independent. On the other hand, when the misalignment effect is included in the simulation, fibre behaviour is conditioned by matrix stress evolution. When matrix reaches its limit stress, fibre stiffness decreases as matrix capacity to restrain fibres from increasing their initial misalignment is reduced due to damage. Fibre stiffness reduction increases as damage in matrix evolves and, when matrix cannot restrain fibres any more, the composite reaches its compression limit strength due to fibre buckling. Thus, fibre stress evolution has a strong dependence on matrix behaviour when it has reached its limit stress.

5 CONCLUSIONS

It has been demonstrated that the S/P rule of mixtures is an appropriate numerical tool to simulate FRP reinforcements of concrete structures, this paper presents a new formulation (to be included in the rule of mixtures algorithm) which takes into account the micro-structural behaviour of fibre reinforced composites to obtain their compression strength. The formulation considers fibre initial misalignments and its evolution along the loading process to obtain the behaviour of fibre and matrix material. The mechanical performance of each one of these components is used to compute the composite behaviour using the serial/parallel rule of mixtures.

Three different simulations, corresponding to different composites, have been performed and the compression strength obtained for each one has been compared with experimental results. This comparison has proved the good performance of the proposed formulation, and its dependence on the composite components characteristics. These simulations have also proven that the new formulation is able to obtain the post-critical evolution of the composite material once fibre buckling has occurred.

ACKNOWLEDGEMENTS

This work has been supported by C.E.E.-FP6 (LESSLOSS project, Ref. FP6-505448(GOCE)); and Ministerio de Ciencia y Tecnología (RECOMP project, Ref. BIA2005-06952; DECOMAR project, Ref: MAT2003-09768-C03-02). The fellowship of one of its authors has been provided by CIMNE.

REFERENCES

[1] Rabinovitch, O., “Nonlinear (buckling) effects in RC beams strengthened with composite materials subjected to compression”, *I. J. Solids and Structures*, 41, 20, 2004, pp 5677-5695

[2] Rosen, B., *Fibre composite materials*, ASM Metals Park, Ohio, USA, 1965, pp 37-45

[3] Barbero, E.J., Tomblin, J.S., “A damage mechanics model for compression strength of composites”, *I. J. Solids and Structures*, 33, 29, 1996, pp 4379-4393

[4] Balacó de Morais, A., Torres Marques, A., “A micromechanical model for the prediction of the lamina longitudinal compression strength of composite laminates”, *J. of Composite Materials*, 31, 14, 1997, pp 1397-1412

[5] Drapier, S., Grandidier, J.C., Potier-Ferry, M., “Towards a numerical model of the compressive strength for long fibre composites”, *E. J. Mechanics A/Solids*, 18, 1, 1999, pp 69-92

[6] Jochum, C., Grandidier, J.C., “Microbuckling elastic modelling approach of a single carbon fibre embedded in an epoxy matrix”, *Composites and Science Technology*, 64, 16, 2004, pp 2442-2449

[7] Rastellini, F., *Modelización numérica de la no-linealidad constitutive de laminados compuestos* PhD thesis, RMEE, UPC, 2006

[8] Martinez, X., Oller, S., Barbat, A., “Numerical tool to study structural reinforcement of steel reinforced concrete (RC) structures under seismic loads using fibre reinforced polymers (FRP)”, *ECEES-1 Proceedings*, Geneva, Switzerland, Sept. 2006.

[9] Trusdell, C., Toupin, R., *The classical field theories*, Handbuch der physik iii/i, Springer Verlag, Berlin, Germany, 1960.

[10] Spadea, G., Benicardino, F., Swamy, R., “Structural behaviour of composite RC beams with externally bonded CFRP”, *J Composites for Construction,* 2, 3, 1998, pp 132-137

[11] Hetényi, M., *Beams on elastic foundation. Theory with applications in the field of civil and mechanical engineering*, Ann Arbor: The University of Michigan Press, Michigan, USA, 1971